





Calorimetric Studies of Magnesium-Rich Mg-Pd Alloys

Adam Dębski¹, Sylwia Terlicka¹, Władysław Gašior¹, Wojciech Gierlotka², Magda Pęska³,
Julita Dworecka-Wójcik³ and Marek Polański^{3,*}

¹ Institute of Metallurgy and Materials Science, Polish Academy of Sciences, 25 Reymonta Street, 30-059 Cracow, Poland; a.debski@imim.pl (A.D.); s.terlicka@imim.pl (S.T.); w.gasior@imim.pl (W.G.)

² Department of Materials Science and Engineering, National Dong Hwa University, Shoufong 974, Taiwan; wojtek@gms.ndhu.edu.tw

³ Department of Functional Materials and Hydrogen Technology, Military University of Technology, 2 Kaliskiego St., 00-908 Warsaw, Poland; magda.peska@wat.edu.pl (M.P.); julita.dworecka@wat.edu.pl (J.D.-W.)

* Correspondence: marek.polanski@wat.edu.pl

Abstract: Solution calorimetry with liquid aluminum as the bath was conducted to measure the enthalpy of a solution of magnesium and palladium as well as the standard formation enthalpies of selected magnesium-palladium alloys. These alloys were synthesized from pure elements, which were melted in a resistance furnace that was placed in a glove box containing high-purity argon and a very low concentration of impurities, such as oxygen and water vapor. A Setaram MHTC 96 Line evo drop calorimeter was used to determine the energetic effects of the solution. The enthalpies of the Mg and Pd solutions in liquid aluminum were measured at 1033 K, and they equaled -8.6 ± 1.1 and -186.8 ± 1.1 kJ/mol, respectively. The values of the standard formation enthalpy of the investigated alloys with concentrations close to the Mg_6Pd , ϵ , Mg_5Pd_2 , and Mg_2Pd intermetallic phases were determined as follows: -28.0 ± 1.2 kJ/mol of atoms, -32.6 ± 1.6 kJ/mol of atoms, -46.8 ± 1.4 kJ/mol of atoms, and -56.0 ± 1.6 kJ/mol of atoms, respectively. The latter data were compared with existing experimental and theoretical data from the literature along with data calculated using the Miedema model.

Keywords: formation enthalpy; drop calorimetry; solution in aluminum bath; Mg-Pd alloys



Citation: Dębski, A.; Terlicka, S.; Gašior, W.; Gierlotka, W.; Pęska, M.; Dworecka-Wójcik, J.; Polański, M. Calorimetric Studies of Magnesium-Rich Mg-Pd Alloys. *Materials* **2021**, *14*, 680. <https://doi.org/10.3390/ma14030680>

Academic Editor:

Haralampos N. Miras

Received: 27 December 2020

Accepted: 29 January 2021

Published: 2 February 2021

Publisher's Note: MDPI stays neutral with regard to jurisdictional claims in published maps and institutional affiliations.



Copyright: © 2021 by the authors. Licensee MDPI, Basel, Switzerland. This article is an open access article distributed under the terms and conditions of the Creative Commons Attribution (CC BY) license (<https://creativecommons.org/licenses/by/4.0/>).

1. Introduction

Energy is a very important commodity in life. Most energy still comes from natural sources, such as coal and oil, but scientists all over the world are constantly searching for an alternative, renewable, and efficient energy source to reduce the climate change caused by the combustion products of natural fuels, which have a negative impact on the climate [1]. Hydrogen is the best-known chemical energy carrier that can be very effectively converted to electricity in Proton-Exchange Membrane Fuel Cells with only water and heat generation. The main problem scientists are trying to solve is finding a suitable material for hydrogen storage with the possibility of the fast absorption and desorption of hydrogen, especially in applications for mobile devices [2–4].

Research on solid-state hydrogen storage materials has been conducted for many years. Some of these materials are metals and their alloys and are capable of reversibly absorbing large amounts of hydrogen. Magnesium has been studied extensively for applications as a hydrogen storage material because magnesium hydride, which Mg creates as it reacts with hydrogen, has a high gravimetric and volumetric density of hydrogen storage (7.6 mass % and 110 g H/L, respectively) [5–7]. However, its high enthalpy of decomposition requires high operating temperatures for the desorption of hydrogen, while the slow diffusion kinetics of hydrogen by mass, for example, poses challenges for its large-scale deployment. To overcome these difficulties, small amounts of additives are added to magnesium to create magnesium compounds, which, in relation to pure Mg, improves the unfavorable

thermodynamics and sometimes the kinetics of the reaction [8]. Significant improvements were made in this field in order to modify the thermodynamics of Mg-based systems starting more than 50 years ago [9,10], but the research in this area is continuing, including alloying with transition [11–17] catalysts [18,19], complex hydride additives [20], and even mechanical processing [21–23]. It has been indicated that the addition of noble metals, such as palladium or silver, can enhance the storage properties of magnesium [16,24–27]. Despite this, the thermodynamics and phase diagrams for magnesium systems such as Mg-Pd and Mg-Pt (and others) are limited and sometimes incomplete; this knowledge is necessary for designing and producing proper materials.

The phase diagram of the Mg-Pd system was estimated for the first time by Nayeb-Hashemi and Clark [28]. It was based on limited data presented by [29–31] and contained five uncertain intermetallic phases (Mg_6Pd , Mg_4Pd , Mg_5Pd_2 , $MgPd$, and $Mg_{0.9}Pd_{1.1}$).

Next, based on their own experimental data from differential thermal analysis (DTA) for Pd alloys for the composition range between 0 and 56 at.%, Makongo et al. [32] presented a new variant of the binary system which was quite different from what Nayeb-Hashemi and Clark [28] proposed. The last version of the Mg-Pd system was published by Okamoto [33] and is reproduced in Figure 1.

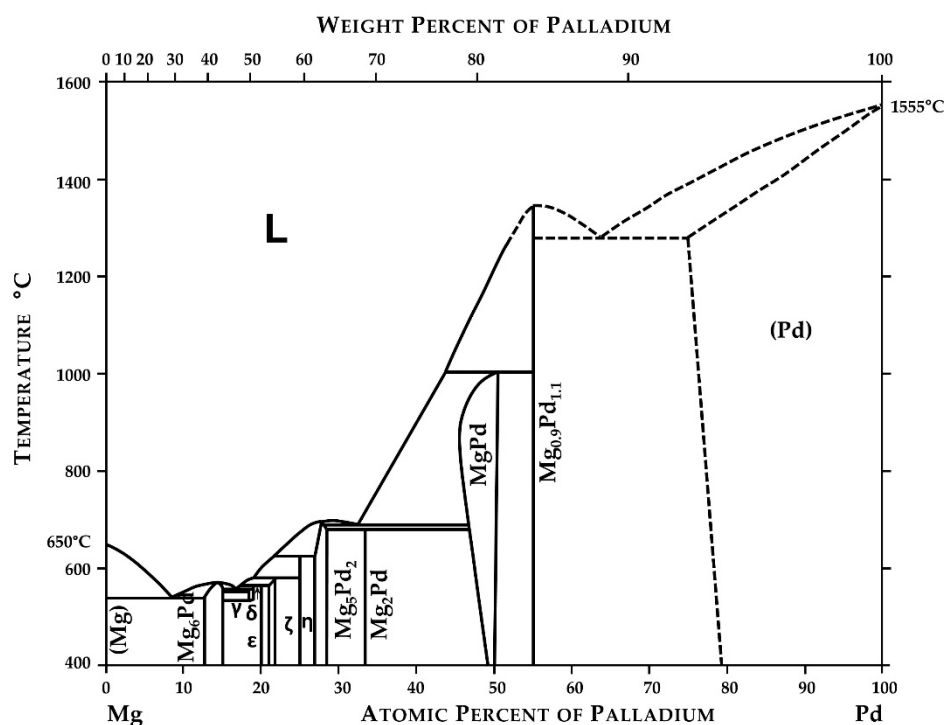


Figure 1. Phase diagram of the Mg-Pd system. Reprinted with permission from ref. [33]. 2010, Springer Nature.

The calculations of the formation energy for the Mg_6Pd , $Mg_{57}Pd_{13}$, Mg_3Pd , Mg_5Pd_2 , and $MgPd$ intermetallic phases were conducted and published by Fernandez et al. [34,35]. The first experimental values of the formation enthalpy of the Mg_6Pd and Mg_5Pd_2 intermetallic compounds were measured by Delsante et al. [36] using direct drop calorimetry, and they were equal to -28.2 ± 1.0 and -39.5 ± 2.8 kJ/mol of atoms, respectively. The formation enthalpies of six Mg-rich alloys corresponding to intermetallic phases from the Mg-Pd system were also presented in our previous work [37]. They were investigated using solution calorimetry in a liquid tin bath, and the determined formation energies equaled -27.0 ± 0.8 , -34.4 ± 0.9 , -35.2 ± 1.4 , -44.2 ± 0.9 , -46.0 ± 0.7 , and -54.3 ± 2.3 kJ/mol of atoms for alloys containing 14.6 at.% Pd, 19.4 at.% Pd, 20.1 at.% Pd, 27.7 at.% Pd, 29.3 at.% Pd, and 35.5 at.% Pd, respectively. Moreover, the ab initio calculations of the formation

energies of all existing intermetallic phases shown in Figure 1 were also reported in our other work [38].

This work is a continuation of research on the thermodynamic properties of the Mg-Pd system initiated by our group. This paper presents an extension of the results of the formation enthalpies of Mg-rich alloys which correspond to intermetallic phases. During the calorimetric measurements, different types of metallic baths were used. The choice of bath is determined by its ability to dissolve the test components forming the alloy during the test. In addition, the bath should have a low melting point, negligible evaporation pressure in the temperature range chosen for tests, and a lower density (as compared to the tested specimen) to prevent the sample from floating on the surface of the liquid bath. For many years, molten tin was used as the main solvent in the calorimetric measurements. However, liquid tin was not always is the best possible solvent for dissolving transition metals, as discussed by Colinet in [39]. In the case of the mentioned research group, liquid aluminum is often used. Despite the fact that the formation enthalpy is a physical value and theoretically should not be affected by the bath type, in practice the measured value is affected by measurement conditions. For these reasons, the presented investigations were conducted by solution calorimetry using a liquid aluminum bath in order to compare the obtained results with previous measurements.

2. Materials and Methods

Table 1 contains a list of the materials that were applied to determine the standard enthalpies of the formation of the investigated alloys. These alloys were prepared in a glove box (Labmaster, MBraun, Garching, Germany) in a high-purity argon atmosphere ($\text{H}_2\text{O} < 0.5$ ppm, $\text{O}_2 < 0.1$ ppm, N_2 was not monitored and was absorbed by Ti at 1100 K). Calculated and weighted (0.1 mg precision) amounts of metals (Pd and Mg) were melted in a resistance furnace in stainless steel crucibles (AISI 304L, Accelor Mittal, Luxembourg). After melting and careful stirring, the liquid alloys were poured into a specially designed steel ingot mold. Finally, the obtained alloys were annealed at 663 K for 72 and 84 h (Table 2) in the furnace that was placed in the glove box containing the protective atmosphere characterized above.

Table 1. Specifications of the applied materials.

Chemical Name	Source	Purity (Mass %)	Analysis Method
Magnesium	Sigma Aldrich	99.9	Certified purity
Palladium	Safina a.s.	99.95	Certified purity
Argon	Air Products	99.9999	Certified purity

Table 2. Homogenization conditions of the prepared alloys.

No.	Alloys (Phases)	Annealing Temperature	Annealing Time (h)
1	14.6 at.% Pd	663	84
2	19.4 at.% Pd	663	84
3	29.3 at.% Pd	663	72
4	35.5 at.% Pd	663	72

The structural studies of the presented Mg-Pd alloys were conducted after the homogenization process with the use of X-ray diffraction (Ultima IV; Rigaku, Tokyo, Japan; $\text{Co K}\alpha$ radiation source; 1.79026 Å) and SEM/EDS (FEI Quanta 3D SEM). A full description of these results was presented in our previous work [37], and both the results of phase analyses and SEM observations are shown in the Supplementary Materials, Figures S1–S4.

The calorimetric studies were performed in a protective argon atmosphere with the use of a Setaram MHTC 96 line evo drop calorimeter using alumina crucibles. The conducted calorimetric studies were similar to our previous calorimetric measurements presented

in [40–42]. Before each experiment began, the workspace of the calorimeter was purified by evacuation with a vacuum pump and flushed with high-purity argon. Next, the calibration constant was determined using six pieces of Al.

The enthalpy of the formation ($\Delta_f H$) values of the measured phases at 298 K were calculated from the difference in the heat effects, which corresponded to heating the samples from room temperature (298 K) to the measurement temperature (1033 K) and observing the dissolution of the studied phases and their components in the aluminum bath. The $\Delta_f H$ values were computed using the following equation:

$$\Delta_f H = x_{\text{Mg}} \Delta H_{\text{Mg}}^0 + x_{\text{Pd}} \Delta H_{\text{Pd}}^0 - \Delta H_{x_{\text{Mg}}x_{\text{Pd}}}^0 \quad (1)$$

where $\Delta_f H$ is the enthalpy of the formation of the measured phase; x_{Mg} and x_{Pd} are the mole fractions of the components, respectively; and ΔH_{Mg}^0 , ΔH_{Pd}^0 , and $\Delta H_{x_{\text{Mg}}x_{\text{Pd}}}^0$ are the heat effects accompanying the dissolution of one mole of the components (Mg and Pd) and phases in the aluminum bath, respectively. The ΔH_{Mg}^0 and ΔH_{Pd}^0 values are the sums of the limiting partial enthalpy of the solution of liquid Mg and Pd in a liquid Al bath and the enthalpy change of the pure Mg and Pd from room temperature to measurement temperature:

$$\Delta H_{\text{Mg}}^0 = \Delta_{\text{sol}} \overline{H}_{\text{Mg}(l)}^\infty + \Delta H_{\text{Mg}}^{T_{298} \rightarrow T_{1033}} \quad (2)$$

$$\Delta H_{\text{Pd}}^0 = \Delta_{\text{sol}} \overline{H}_{\text{Pd}(l)}^\infty + \Delta H_{\text{Pd}}^{T_{298} \rightarrow T_{1033}} \quad (3)$$

In this study, the heat effects ΔH^{ef} of the dissolution of the binary alloys as well as metals were measured.

3. Results and Discussion

The limiting partial enthalpy of the solution of Mg and Pd in liquid aluminum was measured at the first stage of the calorimetric investigations. The necessary thermochemical data of metals were calculated using Pandat 2013 [43] (Pan SGTE database based on the original SGTE v4.4 database [44]). The experimental results of the limiting partial enthalpy of the solution of Mg and Pd in liquid aluminum are presented in Tables 3 and 4, respectively.

Table 3. Values of the limiting partial enthalpy of the solution of liquid Mg $\Delta_{\text{sol}} \overline{H}_{\text{Mg}(l)}^\infty$ in liquid Al. Atmosphere: argon at a pressure $p = 0.1$ MPa; calibration constant $K = 0.000003207$ kJ/ μ Vs; enthalpy of the pure Mg $\Delta H_{\text{Mg}}^{T_{298} \rightarrow T_{1033}} = 30.0048$ kJ/mol; temperature of the Al bath $T_M = 1033$ K; and drop temperature $T_D = 298$ K.

Measurement No.	Dropped Mass of Samples (g)	At.% of Mg in Al Bath	Heat Effects ΔH^{ef} (kJ/mol)	Limiting Partial Enthalpy of Solution $\Delta_{\text{sol}} \overline{H}_{\text{Mg}(l)}^\infty$ (kJ/mol)
1	0.0225	0.16	21.4	−8.6
2	0.0397	0.45	21.2	−8.8
3	0.0276	0.65	21.6	−8.5
4	0.0414	0.95	21.7	−8.3
Average	-	-	21.5	−8.6
Standard error	-	-	1.1	1.1

The standard enthalpies of the formation of the Mg-Pd alloys were determined by employing solution calorimetry. The obtained results are presented in Table 5 together with the standard errors.

The comparison of the formation enthalpies of the investigated alloys obtained in this study is presented in Figure 2, together with the experimental data obtained from the direct reaction method [36], as well as the results from the ab initio method [34,38] and calculations using the Miedema model [45,46].

Table 4. Values of the limiting partial enthalpy of the solution of liquid Pd $\Delta_{\text{sol}}\overline{H}_{\text{Pd}(l)}^{\infty}$ in liquid Al. Atmosphere: argon at a pressure $p = 0.1$ MPa; a calibration constant $K = 0.000003207$ kJ/ μVs ; enthalpy of the pure Pd $\Delta H_{\text{Pd}}^{T_{298} \rightarrow T_{1033}} = 32.3062$ kJ/mol; temperature of the Al bath $T_M = 1033$ K; and drop temperature $T_D = 298$ K.

Measurement No.	Dropped Amount of Samples (g)	At.% of Pd in Al Bath	Heat Effects ΔH^{ef} (kJ/mol)	Limiting Partial Enthalpy of Solution $\Delta_{\text{sol}}\overline{H}_{\text{Pd}(l)}^{\infty}$ (kJ/mol)
1	0.0822	0.14	−154.6	−186.9
2	0.0850	0.28	−154.1	−186.4
3	0.0860	0.42	−154.4	−186.7
4	0.0894	0.57	−154.7	−187.0
5	0.0861	0.71	−154.6	−186.9
Average	-	-	−154.5	−186.8
Standard deviation	-	-	1.1	1.1

Table 5. Heat effects ΔH^{ef} of the solution and formation enthalpies $\Delta_f H$ of the intermetallic phases from the Mg-Pd system. The temperature of the Al bath was 1033 K.

Alloys	T (K)	Sample No.	ΔH^{ef} (kJ/mol of atoms)	$\Delta_f H$ (kJ/mol of atoms)
14.6 at.% Pd (Mg ₆ Pd)	298	1	24.8	−29.0
		2	23.4	−27.6
		3	22.7	−27.0
		4	23.4	−27.7
		5	25.3	−29.5
		6	22.9	−27.2
		Average Standard error	23.8 1.2	−28.0 1.2
19.4 at.% Pd ~(ϵ)	298	1	19.3	−31.9
		2	21.4	−34.1
		3	19.2	−31.9
		4	20.0	−32.7
		Average Standard error	20.0 1.6	−32.6 1.6
		29.3 at.% Pd ~(Mg ₅ Pd ₂)	298	1
2	16.4			−46.5
3	16.7			−46.8
4	16.3			−46.4
Average Standard error	16.7 1.4			−46.8 1.4
35.5 at.% Pd ~(Mg ₂ Pd)	298			1
		2	16.1	−57.1
		3	14.6	−55.6
		4	13.8	−54.9
		Average Standard error	15.0 1.6	−56.0 1.6

As seen in Figure 2, the addition of palladium affects the lowering of the enthalpy of the formation values of the studied alloys. This trend is observed to $x_{\text{Pd}} = 0.5$, which is also documented by the Miedema model and ab initio calculations. Moreover, the obtained formation enthalpy of the alloy close to the composition of the Mg₆Pd intermetallic phase is in very good agreement with the data measured by the direct reaction method [36], as well as the ab initio calculations [38]. A large discrepancy is observed between the values calculated using the Miedema model [45,46] and the experimental measurements, which reach ~6 kJ/mol of atoms. In the case of the enthalpy of the formation of the alloy in which the concentration is close to the ϵ - intermetallic phase, the results obtained

from the calculations are similar to those obtained from the measurements. In regard to alloys close to the Mg_5Pd_2 phase, the greatest differences in values are observed between those measured by the direct reaction method and those obtained by the solution method (in Al and Sn), and these calculated values fluctuate between 5 and 7 kJ/mol of atoms. One can suppose that several reasons influence the discrepancy between the results from the direct synthesis method and those obtained from the solution method. In the direct reaction method, the reason for this may be the partial reaction of the sample during the preparation of the powders, the oxidation of the powders, and the fact that the reaction in the calorimeter may not be complete during the measurement. Moreover, for the direct method, the XRD studies were performed after the sample had cooled down together with the calorimeter, which allowed the sample to have a longer reaction time. Taking these factors into consideration for the discrepancies obtained with the Mg_5Pd_2 phase, it seems that the dissolution method appears to be more accurate for measuring the remaining palladium-rich phases.

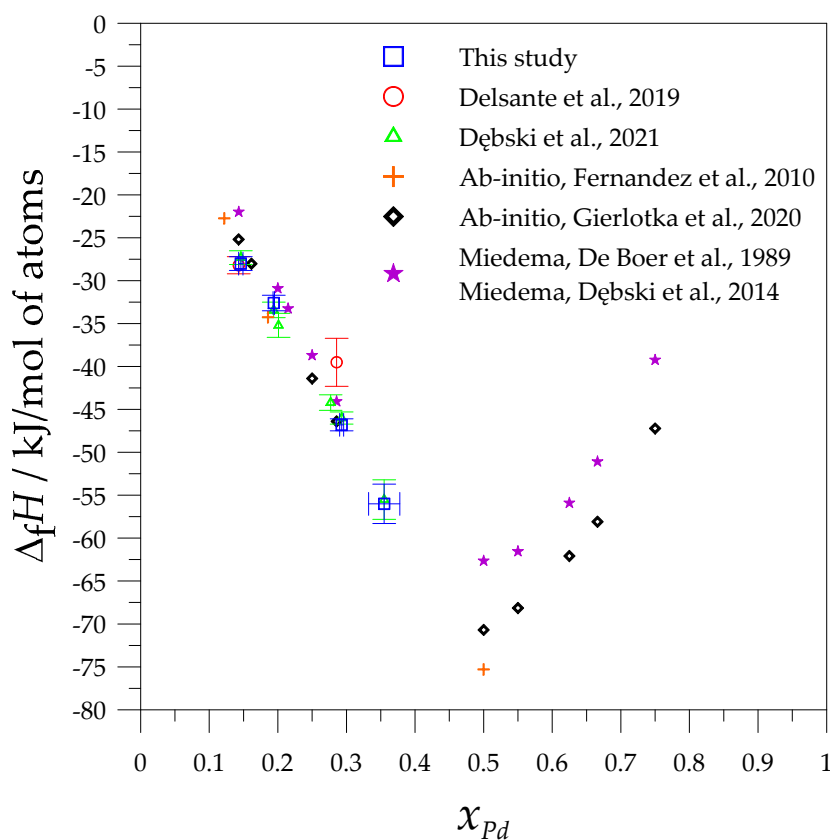


Figure 2. Comparison of the experimental and calculated values of the standard formation enthalpies of the Mg-Pd intermetallic phases and alloys (solution method: in liquid aluminum—this study, in liquid tin (Dębski et al., 2021 [37]), direct reaction method (Delsante et al., 2019 [36]), with ab initio calculations (Fernandez et al., 2010 [34]; Gierlotka et al., 2020 [38]) and the Miedema model (De Boer et al., 1989 [45]; Dębski et al., 2014 [46]).

Similar observations have been reported by Rzyman et al. [47], who compared the enthalpies of the formation of intermetallic phases from the Al-Ti system obtained by the direct reaction and solution calorimetric methods. Only in the case of the Al_3Ti phase were the results obtained from both calorimetric methods in good agreement, while for the remaining phases from the Al-Ti system the differences were about 5 kJ/mol of atoms for the AlTi phase and about 10 kJ/mol of atoms for the AlTi_3 phase. Moreover, it was proven that, during the reaction of titanium and aluminum powders, the first obtained product was the Al_3Ti phase, regardless of the applied proportion. For this reason, the data for the

enthalpy of formation for the Al₃Ti phase obtained from both methods are consistent. In the case of the AlTi and AlTi₃ phases, the observed differences in the enthalpy of formation values indicate that the reaction of phase formation was not completed in the calorimeter, and this is the reason for the differences in the results obtained from the two methods.

4. Conclusions

This paper presents experimental data of the limiting partial enthalpy of a solution of magnesium and palladium in liquid aluminum at 1033 K, as well as the standard formation enthalpy values of four alloys with chemical compositions close to the Mg₆Pd, ϵ , Mg₅Pd₂, and Mg₂Pd intermetallic phases that were measured by solution calorimetry a liquid aluminum bath. The obtained data for the limiting partial enthalpy of a solution of Pd and Mg in liquid aluminum can be used in future studies of phases and alloys containing these metals in their composition.

The obtained value for the formation enthalpy of the alloy close to the Mg₆Pd intermetallic phase agrees well with both the values obtained by the solution calorimetry in liquid Sn and direct reaction methods.

In the case of an alloy with a composition very close to the Mg₅Pd₂ intermetallic phase, the $\Delta_f H$ values determined by both solution calorimetry methods are similar and more exothermic than the data obtained by the direct reaction method.

Moreover, data on the standard enthalpies of formation of the Mg-Pd solid phases measured by solution calorimetry showed a slightly better correlation with those obtained by the ab initio calculations than those calculated by the Miedema model.

The calculated formation enthalpies of the Mg-Pd phases and alloys by the ab initio method were more exothermic in comparison to those calculated by the Miedema model, and the observed differences varied between 5 and 15 kJ/mol of atoms.

Supplementary Materials: The following are available online at <https://www.mdpi.com/1996-1944/14/3/680/s1>, Figure S1. X-Ray diffraction pattern (Co anode $\lambda = 1.78 \text{ \AA}$) and SEM (BSE) image of Alloy 1. Figure S2. X-Ray diffraction pattern (Co anode $\lambda = 1.78 \text{ \AA}$) and SEM (BSE) image of Alloy 2. Figure S3. X-Ray diffraction pattern (Co anode $\lambda = 1.78 \text{ \AA}$) and SEM (BSE) image of Alloy 3. Figure S4. X-Ray diffraction pattern (Co anode $\lambda = 1.78 \text{ \AA}$) and SEM (BSE) image of Alloy 4.

Author Contributions: A.D.: Conceptualization, investigation, writing, supervision. S.T.: Investigation. W.G. (Władysław Gašior): Supervision. W.G. (Wojciech Gierlotka): Investigation, Methodology. M.P. (Magda Peška): discussion, visualization. J.D.-W.: verification, discussion. M.P. (Marek Polański): supervision. All authors have read and agreed to the published version of the manuscript.

Funding: This work is supported by the National Science Centre, Poland, for funding Project No. 2018/31/B/ST8/01371 in the years 2019–2022, as a continuation of research on materials for hydrogen storage initiated at the National Center for Research and Development, Poland by research, carried out in the ZAMAT project POIG 01.01.02-00-015/09. The support of the statutory research funds of Department of Functional Materials and Hydrogen Technology, Military University of Technology is appreciated.

Institutional Review Board Statement: Not applicable.

Informed Consent Statement: Not applicable.

Data Availability Statement: The data that support the findings of this study are available from the corresponding author, [A.D.], upon reasonable request.

Conflicts of Interest: The authors declare no conflict of interest.

References

- Schlapbach, L.; Züttel, A. Hydrogen-Storage Materials for Mobile Applications. *Nature* **2002**, *414*, 353–358. [[CrossRef](#)] [[PubMed](#)]
- Moradi, R.; Groth, K.M. Hydrogen Storage and Delivery: Review of the State of the Art Technologies and Risk and Reliability Analysis. *Int. J. Hydrog. Energy* **2019**, *44*, 12254–12269. [[CrossRef](#)]
- Rivard, E.; Trudeau, M.; Zaghbi, K. Hydrogen Storage for Mobility: A Review. *Materials* **2019**, *12*, 1973. [[CrossRef](#)] [[PubMed](#)]

4. Hadjixenophontos, E.; Dematteis, E.M.; Berti, N.; Wołczyk, A.R.; Huen, P.; Brighi, M.; Le, T.T.; Santoru, A.; Payandeh, S.; Peru, F. A Review of the MSCA ITN ECOSTORE—Novel Complex Metal Hydrides for Efficient and Compact Storage of Renewable Energy as Hydrogen and Electricity. *Inorganics* **2020**, *8*, 17. [[CrossRef](#)]
5. Crivello, J.-C.; Dam, B.; Denys, R.; Dornheim, M.; Grant, D.; Huot, J.; Jensen, T.R.; De Jongh, P.; Latroche, M.; Milanese, C. Review of Magnesium Hydride-Based Materials: Development and Optimisation. *Appl. Phys. A* **2016**, *122*, 97. [[CrossRef](#)]
6. Prabhukhot, P.R.; Wagh Mahesh, M.; Gangal Aneesh, C. A Review on Solid State Hydrogen Storage Material. *Adv. Energy Power* **2016**, 11–22. [[CrossRef](#)]
7. Baran, A.; Polański, M. Magnesium-Based Materials for Hydrogen Storage—A Scope Review. *Materials* **2020**, *13*, 3993. [[CrossRef](#)]
8. Webb, C.J. A Review of Catalyst-Enhanced Magnesium Hydride as a Hydrogen Storage Material. *J. Phys. Chem. Solids* **2015**, *84*, 96–106. [[CrossRef](#)]
9. Reilly, J.J., Jr.; Wiswall, R.H., Jr. The Reaction of Hydrogen with Alloys of Magnesium and Copper1. *Inorg. Chem.* **1967**, *6*, 2220–2223. [[CrossRef](#)]
10. Reilly, J.J., Jr.; Wiswall, R.H., Jr. Reaction of Hydrogen with Alloys of Magnesium and Nickel and the Formation of Mg₂NiH₄. *Inorg. Chem.* **1968**, *7*, 2254–2256. [[CrossRef](#)]
11. Fadonougbo, J.O.; Jung, J.-Y.; Suh, J.-Y.; Lee, Y.-S.; Shim, J.-H.; Cho, Y.W. Low Temperature Formation of Mg₂FeH₆ by Hydrogenation of Ball-Milled Nano-Crystalline Powder Mixture of Mg and Fe. *Mater. Des.* **2017**, *135*, 239–245. [[CrossRef](#)]
12. Fadonougbo, J.O.; Jung, J.-Y.; Suh, J.-Y.; Lee, Y.-S.; Shim, J.-H.; Fleury, E.; Cho, Y.W. The Role of Fe Particle Size and Oxide Distribution on the Hydrogenation Properties of Ball-Milled Nano-Crystalline Powder Mixtures of Fe and Mg. *J. Alloys Compd.* **2019**, *806*, 1039–1046. [[CrossRef](#)]
13. Sun, Z.; Lu, X.; Nyahuma, F.M.; Yan, N.; Xiao, J.; Su, S.; Zhang, L. Enhancing Hydrogen Storage Properties of MgH₂ by Transition Metals and Carbon Materials: A Brief Review. *Front. Chem.* **2020**, *8*, 552. [[CrossRef](#)]
14. Dufour, J.; Huot, J. Rapid Activation, Enhanced Hydrogen Sorption Kinetics and Air Resistance in Laminated Mg–Pd 2.5 at.%. *J. Alloys Compd.* **2007**, *439*, 5–7. [[CrossRef](#)]
15. Huot, J.; Enoki, H.; Akiba, E. Synthesis, Phase Transformation, and Hydrogen Storage Properties of Ball-Milled TiV_{0.9}Mn_{1.1}. *J. Alloys Compd.* **2008**, *453*, 203–209. [[CrossRef](#)]
16. Huot, J.; Yonkeub, A.; Dufour, J. Rietveld Analysis of Neutron Powder Diffraction of Mg₆Pd Alloy at Various Hydriding Stages. *J. Alloys Compd.* **2009**, *475*, 168–172. [[CrossRef](#)]
17. Fadonougbo, J.O.; Kim, H.-J.; Suh, B.-C.; Suh, J.-Y.; Lee, Y.-S.; Shim, J.-H.; Yim, C.D.; Cho, Y.W. Kinetics and Thermodynamics of Near Eutectic Mg–Mg₂Ni Composites Produced by Casting Process. *Int. J. Hydrogen Energy* **2020**, *45*, 29009–29022. [[CrossRef](#)]
18. Ouyang, L.; Liu, F.; Wang, H.; Liu, J.; Yang, X.-S.; Sun, L.; Zhu, M. Magnesium-Based Hydrogen Storage Compounds: A Review. *J. Alloys Compd.* **2020**, 832. [[CrossRef](#)]
19. Crivello, J.C.; Denys, R.V.; Dornheim, M.; Felderhoff, M.; Grant, D.M.; Huot, J.; Jensen, T.R.; de Jongh, P.; Latroche, M.; Walker, G.S.; et al. Mg-Based Compounds for Hydrogen and Energy Storage. *Appl. Phys. A* **2016**, *122*. [[CrossRef](#)]
20. Pistidda, C. Metals in Hydrogen Technology. *Metals* **2020**, *10*, 456. [[CrossRef](#)]
21. Floriano, R.; Leiva, D.R.; Melo, G.C.; Ishikawa, T.T.; Huot, J.; Kaufman, M.; Figueroa, S.J.A.; Mendoza-Zélis, L.A.; Damonte, L.C.; Botta, W.J. Low Temperature Rolling of AZ91 Alloy for Hydrogen Storage. *Int. J. Hydrogen Energy* **2017**, *42*, 29394–29405. [[CrossRef](#)]
22. Skryabina, N.; Aptukov, V.; Romanov, P.; Fruchart, D.; de Rango, P.; Girard, G.; Grandini, C.; Sandim, H.; Huot, J.; Lang, J.; et al. Microstructure Optimization of Mg-Alloys by the ECAP Process Including Numerical Simulation, SPD Treatments, Characterization, and Hydrogen Sorption Properties. *Molecules* **2018**, *24*, 89. [[CrossRef](#)]
23. Huot, J.; Tournant, M. Effect of Cold Rolling on Metal Hydrides. *Mater. Trans.* **2019**, *60*, 1571–1576. [[CrossRef](#)]
24. Xin, G.; Yang, J.; Fu, H.; Li, W.; Zheng, J.; Li, X. Excellent Hydrogen Sorption Kinetics of Thick Mg–Pd Films under Mild Conditions by Tailoring Their Structures. *R. Soc. Chem.* **2013**, *3*, 4167–4170. [[CrossRef](#)]
25. Urretavizcaya, G.; Sarmiento Chávez, A.C.; Castro, F.J. Hydrogen Absorption and Desorption in the Mg–Ag System. *J. Alloys Compd.* **2014**, *611*, 202–209. [[CrossRef](#)]
26. Si, T.Z.; Zhang, J.B.; Liu, D.M.; Zhang, Q.A. A New Reversible Mg₃Ag–H₂ System for Hydrogen Storage. *J. Alloys Compd.* **2013**, *581*, 246–249. [[CrossRef](#)]
27. Dufour, J.; Huot, J. Study of Mg₆Pd Alloy Synthesized by Cold Rolling. *J. Alloys Compd.* **2007**, *446–447*, 147–151. [[CrossRef](#)]
28. Nayeb-Hashemi, A.A.; Clark, J.B. The Mg–Pd (Magnesium–Palladium) System. *Bull. Alloy Phase Diagr.* **1985**, *6*, 164–167. [[CrossRef](#)]
29. Savitsky, E.M.; Terekhova, V.F.; Birun, N.A. Equilibrium Diagram of the Mg–Pd System. *Russ. J. Inorg. Chem.* **1962**, *7*, 1228–1231.
30. Ferro, R. Research on the Alloys of Noble Metals with the More Electropositive Elements: III. Micrographic and X-ray Examination of Some Magnesium–Platinum Alloys. *J. Less Common Met.* **1959**, *1*, 424–438. [[CrossRef](#)]
31. Kripyakevich, P.I.; Gladyshevskii, E.I. Crystal Structures of Some Compounds of Palladium with Magnesium. *Sov. Phys. Crystallogr.* **1960**, *5*, 552–554.
32. Makongo, J.P.A.; Prots, Y.; Burkhardt, U.; Niewa, R.; Kudla, C.; Kreiner, G. A Case Study of Complex Metallic Alloy Phases: Structure and Disorder Phenomena of Mg–Pd Compounds. *Philos. Mag.* **2006**, *86*, 427–433. [[CrossRef](#)]
33. Okamoto, H. Mg–Pd (Magnesium–Palladium). *J. Phase Equilibria Diffus.* **2010**, *31*, 407–408. [[CrossRef](#)]
34. Fernandez, J.F.; Ares, J.R.; Cuevas, F.; Bodega, J.; Leardini, F.; Sanchez, C. A Thermodynamic Study of the Hydrogenation of the Pseudo-Binary Mg₆Pd_{0.5}Ni_{0.5} Intermetallic Compound. *Intermetallics* **2010**, *18*, 233–241. [[CrossRef](#)]

35. Fernandez, J.F.; Widomb, M.; Cuevas, F.; Ares, J.R.; Bodega, J.; Leardini, F.; Mihalkovi, M.; Sánchez, C. First-Principles Phase Stability Calculations and Estimation of Finite Temperature Effects on Pseudo-Binary $Mg_6(Pd_xNi_{1-x})$ Compounds. *Intermetallics* **2011**, *19*, 502–510. [[CrossRef](#)]
36. Delsante, S.; Novakovic, R.; Gagliolo, A.; Borzone, G. Thermodynamic Investigation on the Mg–Pd Intermetallic Phases. *J. Chem. Thermodyn.* **2019**, *139*, 1–8. [[CrossRef](#)]
37. Dębski, A.; Peška, M.; Dworecka-Wójcik, J.; Terlicka, S.; Gašior, W.; Gierlotka, W.; Polański, M. Structural and Calorimetric Studies of Magnesium-Rich Mg-PD alloys. *J. Alloys Compd.* **2021**, *858*. [[CrossRef](#)]
38. Gierlotka, W.; Dębski, A.; Terlicka, S.; Gašior, W.; Peška, M.; Polański, M. Insight into Phase Stability in the Mg–Pd System: The Ab Initio Calculations. *J. Phase Equilibria Diffus.* **2020**, *41*, 681–686. [[CrossRef](#)]
39. Colinet, C. High Temperature Calorimetry: Recent Developments. *J. Alloys Compd.* **1995**, *220*, 76–87. [[CrossRef](#)]
40. Dębski, A.; Dębski, R.; Gašior, W.; Góral, A. Formation Enthalpy of Intermetallic Phases from Ag–Ca System. Experiment vs. Modeling. *J. Alloys Compd.* **2014**, *610*, 701–705. [[CrossRef](#)]
41. Dębski, A.; Terlicka, S.; Budziak, A.; Gašior, W. Calorimetric and XRD Studies of Ag-Rich Alloys from Ag–Li System. *J. Alloys Compd.* **2018**, *732*, 210–217. [[CrossRef](#)]
42. Dębski, A.; Braga, M.H.; Terlicka, S.; Gašior, W.; Góral, A. Formation Enthalpy of Ga–Li Intermetallic Phases. Experiment vs. Calculations. *J. Chem. Thermodyn.* **2018**, *124*, 101–106. [[CrossRef](#)]
43. Chen, S.L.; Daniel, S.; Zhang, F.; Chang, Y.A.; Yan, X.-Y.; Xie, F.-Y.; Schmid-Fetzer, R.; Oates, W.A. The PANDAT Software Package and Its Applications. *Calphad Comput. Coupling Phase Diagr. Thermochem.* **2002**, *26*, 175–188. [[CrossRef](#)]
44. Dinsdale, A.T. SGTE Data for Pure Elements. *Calphad* **1991**, *15*, 317–425. [[CrossRef](#)]
45. De Boer, F.R.; Boom, R.; Mattens, W.C.M.; Miedema, A.R.; Niessen, A.K. *Cohesion in Metals: Transition Metal Alloys (Cohesion and Structure)*; Elsevier: Amsterdam, The Netherlands, 1989.
46. Dębski, A.; Dębski, R.; Gašior, W. New Features of ENTALL Database: Comparison of Experimental and Model Formation Enthalpies. *Arch. Metall. Mater.* **2014**, *59*, 1337–1343. [[CrossRef](#)]
47. Rzyman, K.; Moser, Z.; Gachon, J.C. Calorimetric Studies of the Enthalpies of Formation of Al_3Ti , $AlTi$, $AlTi_3$ and Al_2Ti Compounds. *Arch. Metall. Materials* **2004**, *49*, 545–563.